

Precrack Hysteresis Energy in Determining Its Ductile–Brittle Transition. III. Effect of Temperature

FENG-CHIH CHANG* and HON-CHUN HSU

Institute of Applied Chemistry, National Chiao-Tung University, Hsinchu, Taiwan, Republic of China

SYNOPSIS

A temperature variable has been used to correlate the precrack hysteresis energy and the corresponding ductility in terms of ductile–brittle transition behavior for polycarbonate. When the precrack plastic zone exceeds a critical value, crack extension thereafter will be effectively contained within the domain of the plastic zone and result in ductile fracture. Whether a specimen will fail in a ductile mode or a brittle mode is actually already being decided before the onset of crack initiation. The precrack elastic storage energy, total input energy minus hysteresis energy, is the major driving force to strain the crack tip for crack initiation. A higher testing temperature with lower yield stress converts a greater fraction of the input energy into the precrack hysteresis energy and relieves the storage strain energy available for crack initiation. A polycarbonate-toughening mechanism of increasing temperature is very similar to the presence of rubber by reducing yield stress and increasing the precrack plasticity. © 1994 John Wiley & Sons, Inc.

INTRODUCTION

The ductile–brittle transition temperature (DBTT) has been used to characterize the mechanical behavior of metals for some time. At the DBTT, both ductile and brittle failures are possible in specimens with identical geometry and testing conditions. This definition has been transferred to polymeric materials with various degrees of success. DBTT is not a single temperature as pointed out by Andrews,¹ but, rather, a temperature range, and the size of this range varies from material to material and with the testing method. The same material, such as polycarbonate, can have significantly lower and broad DBTT from tensile or falling weight impact testing (unnotched) than from notched Izod or Charpy impact testing.

Polymeric materials can be classified into two main types: brittle and pseudoductile.² This pseudoductile polymer may fail either brittle (crazing) or ductile (yielding) depending on test conditions and specimen geometry. Pseudoductile polymers,

such as PC and nylon, tend to fail by yielding and have high crack initiation energy (high unnotched toughness) and low propagation energy (low notched toughness). To simplify, the ductile–brittle transition can be considered as being due to a competition between a brittle mechanism (crazing) and a ductile mechanism (yielding). When the yield stress is lower than the crazing stress, a polymer tends to yield and results in ductile fracture. Therefore, the ratio of craze stress and yield stress, σ_z/σ_y , controls the mode of the craze/yield behavior.²

The yield stress σ_y has been shown to be proportional to $\Delta T = T_g - T$ and δ^2 , where T is the testing temperature, and δ^2 , the cohesive energy density.³ The craze stress also decreases with increase of testing temperature but is less sensitive relative to the yield stress. Therefore, the above stress ratio varies with the testing condition and results in either a ductile or brittle mode of failure.

However, such a simple stress competitive mechanism may be applicable under a uniform stress field condition such as tensile testing but is certainly unable to explain the complicated phenomenon of the ductile–brittle transition behavior of the notched specimen since the stress field surrounding the crack tip under deformation is considered inhomogeneous.

* To whom correspondence should be addressed.

Besides, whether a fracture is ductile or brittle, it has to take the whole fracture process into consideration. In rare cases, the fracture mode can change, from the ductile mode to the brittle mode or from the brittle mode to the ductile mode, in the middle of the fracture process. Ward reviewed the behavior of the brittle–ductile transition and characterized it by a critical length $x_{oc} = \alpha GcE/\sigma_y^2$, where α is a number constant whose value is determined by the stress field in the test.⁴ The critical length is the plastic zone size at a general yield of a notch bar and the fracture transition occurs at the temperature (DBTT) at which the quantity $\alpha GcE/\sigma_y^2$ is equal to the critical length in the chosen test.⁴

Polycarbonate, a pseudoductile polymer with lower yield stress than the craze stress under ordinary conditions, has a distinctive ductile–brittle transition in the notched specimens in response to numerous variables such as temperature, thickness, orientation, deformation rate, molecular weight, moisture content, physical aging, notch radius, and elastomer content. It is clear that there is no one overriding mechanism responsible for this behavior and an overall review on this subject was reported in our previous article.⁵ We recently discovered the close relationship between the precrack hysteresis energy and the corresponding ductile–brittle transition behavior that is applicable to essentially all the above-mentioned variables for polycarbonate.^{6–8} We proposed a critical precrack plastic volume in determining whether the failure is in a ductile or brittle mode.^{6–8} The effect of the polycarbonate molecular weight and impact modifier content were the two variables that we previously reported.^{6,7} In this article, we use the same hysteresis concept to explain the criterion of the ductile–brittle transition of polycarbonate based on varying the test temperature. This hysteresis concept can also be extended to determine the critical J (J_c) value in the J -integral fracture mechanics.^{9–11}

EXPERIMENTAL

Natural-grade polycarbonate with a melt flow rate (MFR) of 15 from Dow Chemical Co. was chosen for this study. Procedures including injection molding, slow rate fracture, hysteresis, and scanning electronic microscopy (SEM) were reported previously.^{6,7,12–14} A specially designed chamber equipped with heaters and a liquid nitrogen entry nozzle was used to control the testing temperature.

RESULTS AND DISCUSSION

Theoretical Background

Deforming a notched bar before crack initiation will result in the formation of the crack tip plastic zone. The size of this precrack plastic zone (V_p) is a function of the testing variables, specimen dimension, and material modifications that may include deformation rate (ν), temperature (T), deformation displacement (L), specimen thickness (B), notch radius (r), material yield stress (σ_y), molecular weight (M), directionality (d), moisture content (m), annealing (a), impact modifier or filler content (I), and others:

$$V_p = f(\nu, T, L \cdot B \cdot r, \sigma_y, M, d, m, a, I \cdot \dots) \quad (1)$$

Some of the above variables are not independent but related to others such as temperature and yield stress. Total input energy consists of elastic storage and inelastic hysteresis energy. The contribution of viscoelasticity is considered to be minor under the condition of a very slow deformation rate (10 mm/min) and can be neglected. The approximate inelastic hysteresis energy can be obtained experimentally from the input energy and the corresponding percent hysteresis loss according the following equations:

$$U_t = U_e + U_i = \int F \cdot L \quad (2)$$

$$U_i = \Phi \cdot U_t \quad (3)$$

where U_t , U_e , and U_i are total input energy, elastic storage energy, and inelastic energy, respectively. F is the load and Φ is the percent hysteresis loss. True hysteresis (loss) energy is unobtainable because additional time is necessary to allow for unloading to zero and, therefore, the experimentally obtained hysteresis energy is expected to be higher than the true value. Assume that the plastic energy, U_p , the energy consumed exclusively for the plastic-zone formation, has a relationship with the inelastic energy. The precrack plastic volume is also expected to be yield-stress-related:

$$U_p = K_1 \cdot U_i^n = K_1 (\Phi \cdot U_t)^n \quad (4)$$

$$V_p = K_2 \cdot U_p / \sigma_y^m = K_1 K_2 \cdot \Phi^n \cdot U_t^n / \sigma_y^m \quad (5)$$

where K_1 , K_2 , n , and m , are material constants. At the onset of crack initiation, the deformation displacement $L = L_i$, if

$L_i > L_c$ and $V_p > V_c$, ductile tearing

$L_i \cong L_c$ and $V_p = V_c$, ductile or brittle, or semiductile

$L_i < L_c$ and $V_p < V_c$, brittle

The basic concept of the above description is that a ductile fracture comes from the crack propagation within the domain of the plastic zone. The definition of crack growth, crack propagation, or crack extension used in this article can be ductile tearing if the crack front is within the plastic zone or brittle fracture if the crack front is within the nonplastic zone. Whether a specimen will fail as a ductile mode or a brittle mode is actually already decided before the onset of crack initiation. At onset of crack initiation, if the crack tip plastic zone size is above a critical value, the crack extension later most likely will be contained within the plastic zone and results in ductile failure. The plastic zone will also grow during the process of crack growing as long as the plastic zone front is always ahead of the crack growing front; a complete ductile tearing will result. If the precrack plastic zone has not yet been established to the critical value before the onset of crack initiation, the storage strain energy release from the crack extension will lead the crack front to pass the existing plastic zone front rapidly and the brittle crack front will propagate within the nonplastic region and a brittle fracture occurs. A small crack tip blunting near the root of the notch is always present even in a brittle fractured surface and the distance of this blunting zone depends on the relative ductility or blunting capability. Besides, two small plane-stress ductile yielding zones on both sides but very close to notch root are usually present in a brittle fractured surface.

The above criterion for the brittle-to-ductile brittle transition is generally applicable to polycarbonate with a standard notch (10 mil) and a thinner specimen ($\frac{1}{8}$ in.). Polycarbonate ($\frac{1}{8}$ in. thickness and 10 mil notch) always results in either ductile or brittle failure without any in between (in terms of fracture energy). However, when the notch radius and/or specimen thickness are increased, several unusual types of semiductile modes of fractures have been reported. The Type I semiductile mode is ductile fracture in the front portion (nearly half across the length of the specimen) and brittle fracture in rear portion that has been reported in polycarbonate.^{15,16}

This Type I fracture has been termed the ductile tearing instability, which also occurs on certain rubber-toughened polymer blends.¹⁷

The Type I phenomenon can be interpreted as the crack propagating front passing the plastic zone front in the middle of fracture process and, therefore, it shifts the fracture mode from ductile to brittle. The type II semiductile fracture comes from polycarbonate with a greater notch radius (20 mil) at low temperature (-40°C) where the whole fractured surface is covered with extensive but still localized shear yielding (without the presence of the characteristic lateral contraction of a typical ductile fracture) with fracture energy about the average between ductile and brittle fracture.¹⁸ This Type II phenomenon can be interpreted as the propagating crack front which runs side by side with the plastic zone front; therefore, the crack growth is unable to induce the mass shear yielding with lateral contraction, but, rather, enhances the localized shear yielding mechanism.

When the specimen thickness is increased from $\frac{1}{8}$ to $\frac{1}{4}$ in., the clear presence of both plane-stress (both edges) and plane-strain (central region) may result in an even more complex crack growing pattern. Due to the relatively higher yield stress of the triaxial state, the brittle crack growth advances first and rapidly at the onset of initiation in the central plane-strain region but is eventually held back by the plane-stress yielding already formed on both sides of the specimen and form a triangular mirror brittle zone. The load drops immediately in response to the sudden crack extension and the resultant release of the stored strain energy.

Ductile tearing starts momentarily later from the yielded zones (both sides) and proceeds to the rest of the specimen. This type of fracture can be considered as the Type III semiductile mode except at a lesser degree as the brittle mode and at a higher degree as the ductile mode. This type of fracture was previously reported by Yee¹⁶ and will appear in this article later. However, a typical Type III fracture should possess a clear brittle fracture in the front portion and a ductile fracture in the rear portion of the specimen. This Type III semiductile fracture has been observed on rubber-toughened polycarbonate with a sharper notch that has a V-shape brittle region reflecting the plane-strain restriction.⁸ Our proposed mechanism can also be used to explain Type III fracture as the growing plastic zone front catches up and runs ahead of the brittle crack front and converts the fracture mode from brittle to ductile during the middle of the fracture process.

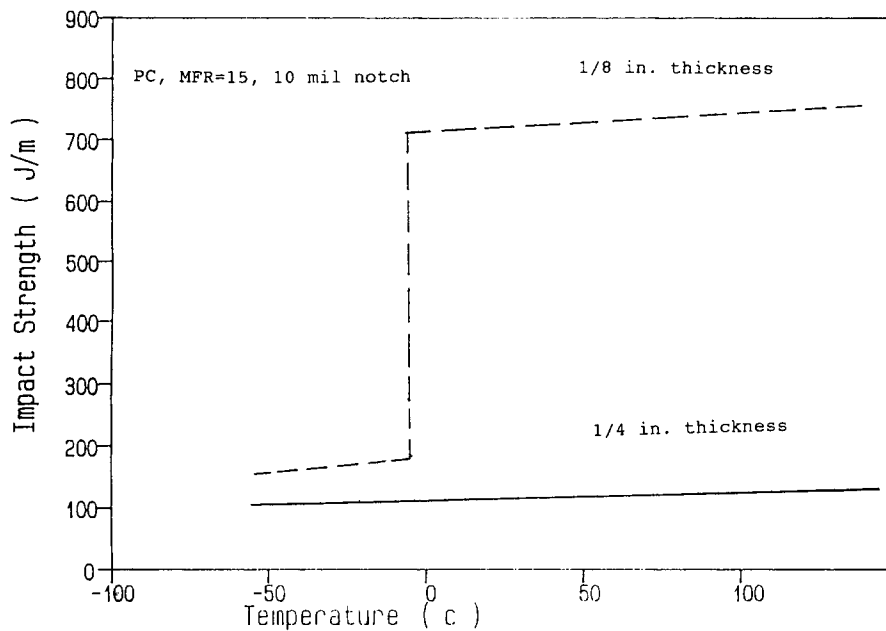


Figure 1 Izod impact strength vs. temperature for polycarbonates with $\frac{1}{8}$ and $\frac{1}{4}$ in. thickness.

A Type IV semiductile fracture has also been identified on $\frac{1}{4}$ in. rubber-toughened polycarbonate where the brittle fracture occurs in the plane-strain central region while ductile fracture occurs on the plane-stress sides.^{8,19} This odd type of fracture (Type IV) can be considered as the ductile tearing front and the brittle crack front grow separately. This proposed critical precrack is able to properly explain most of those unusual types of semiductile fractures.

Effect of Temperature on Izod Impact Strength

A tremendous amount of literature has been reported on this subject and we present only those on polycarbonate with different thicknesses for com-

parison. Figure 1 shows the plots of Izod impact strength vs. temperature on polycarbonate with an MFR = 15 with $\frac{1}{8}$ and $\frac{1}{4}$ in. specimens. Under the impact strain rate (hammer striking velocity is about 3 m/s), the $\frac{1}{8}$ in. specimens have the DBTT at -5°C , whereas the $\frac{1}{4}$ in. specimens have no DBTT since all specimens fail brittle up to 150°C . Temperature is the variable that fails to convert these $\frac{1}{4}$ in. specimens from the brittle to the ductile mode, but other variables, alone or in combination, can, such as reduced strain rate, greater notch radius, higher molecular weight, or addition of impact modifier.

Slow Rate Fracture

This is essentially identical to a standard Izod impact test except that the deformation rate of 10 mm/min was employed and controlled by the Instron. Detailed procedures were reported previously.^{6,12,20} Since all the $\frac{1}{8}$ in. specimens result in ductile fracture, the data will not be presented here. The summarized results from the $\frac{1}{4}$ in. specimens are shown in Figure 2 and Table I. Figure 2 clearly shows that fracture occurs if the testing temperature is 50°C or lower. Crack initiation in most ductile fractures normally occurs prior to the load maximum.^{9,21} For convenience and relative comparison, the load maximum is considered as crack initiation in this article because true initiation of a ductile fracture is difficult to define and to determine.

Table I Slow Rate Notched Fracture Data at Various Temperatures

Temp (°C)	Total Energy (J)	Energy to Max Load (J)	Displacement to Max Load (mm)	Max Load (kN)
0	0.28	0.28	1.76	0.31
25	0.38	0.38	2.15	0.34
50	0.40	0.40	2.20	0.35
75	0.34	0.34	2.06	0.32
75	1.74	0.47	2.50	0.33
75	3.05	0.64	2.77	0.37
100	4.41	0.70	3.77	0.31

Figure 2 shows the DBTT of this material with a specific dimension at 75°C where three possible fracture modes (ductile, semiductile, and brittle) occur. Figure 3 shows that the crack initiation energy increases linearly with increase of crack initiation displacement. Figure 3 clearly demonstrates the importance of crack initiation displacement in dictating the behavior of the resultant fracture, ductile, semiductile, or brittle mode. In general, but not always experimentally, the specimen can resist crack initiation more effectively at higher temperature and results in greater crack initiation displacement and thus is more ductile. Since the portion of the input energy prior to the onset of initiation is consumed as inelastic plastic energy, the precrack plastic zone is expected to be increased with the increase of the deformation displacement. As soon as the precrack deformation displacement or the plastic zone exceeds a certain critical level, any crack developed thereafter will be effectively contained within the domain of the plastic zone and results in ductile tearing as mentioned in the Theoretical Background

section. Figure 3 shows that the critical displacement for the brittle-ductile transition at 75°C is about 2.5 mm, which is slightly lower than the 3.1 mm obtained by varying the polycarbonate molecular weight at an ambient condition.⁶ Lower yield stress due to higher temperature certainly will affect the critical precrack zone and critical initiation displacement.

SEM Morphology

The SEM photographs of the corresponding fractured surfaces are shown in Figure 4(a)-(g). For ductile fracture, the surface appears distorted and irregular with clear lateral constriction. For the brittle fractured surfaces, a crack tip blunting zone and large numbers of brittle-type striating lines are present but show no sign of lateral contraction. A particularly interesting morphology comes from this Type III semiductile fractured surface [Fig. 4(e)] at 75°C. Replotting of this semiductile fractured surface and the corresponding load-displacement

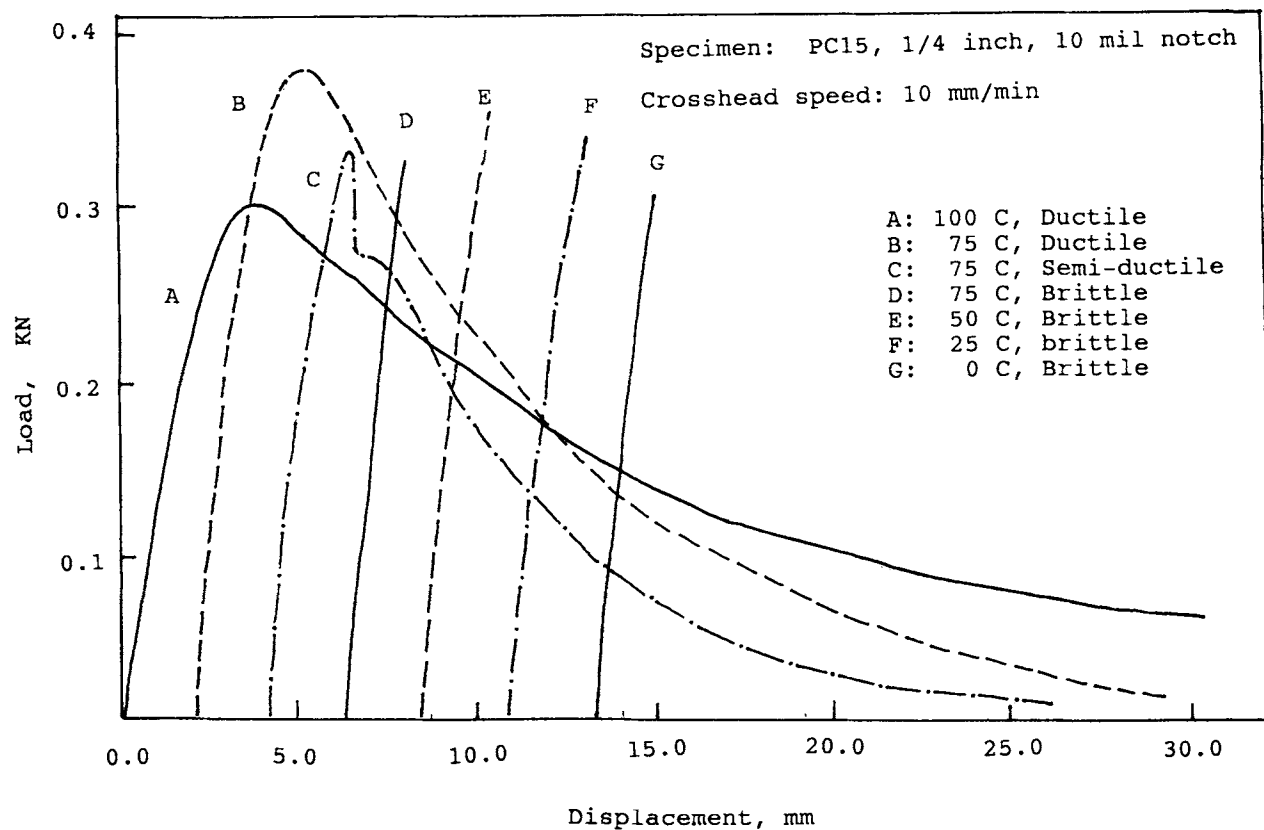


Figure 2 Typical load-displacement curves for polycarbonates, MFR = 15, $\frac{1}{4}$ in. thickness, 10 mil notch, 10 mm/min deformation rate. (A) $T = 100^\circ\text{C}$, ductile; (B) $T = 75^\circ\text{C}$, ductile; (C) $T = 75^\circ\text{C}$, semiductile; (D) $T = 75^\circ\text{C}$, brittle; (E) $T = 50^\circ\text{C}$, brittle; (F) $T = 25^\circ\text{C}$, brittle; (G) $T = 0^\circ\text{C}$, brittle.

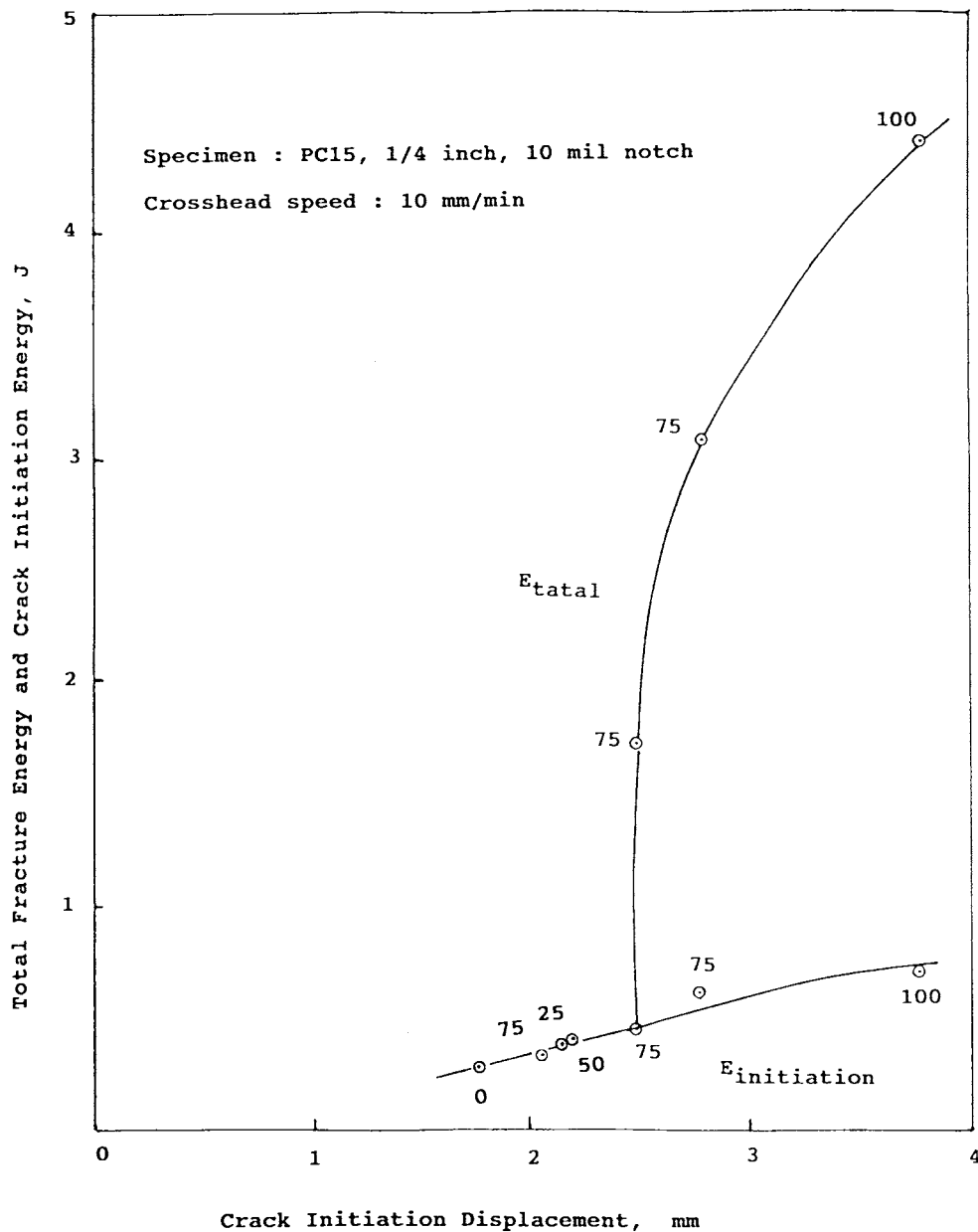


Figure 3 Plots of crack initiation displacement vs. total fracture energy and crack initiation energy for polycarbonate at different temperatures. Data points come from Figure 2.

curve are shown in Figure 5 with various fracture zones defined. Zone I is the crack blunting zone. Zone II is the plane-strain brittle fast crack zone, which corresponds to the sharp load drop shown in the load-displacement curve when the plane-stress regions (on both sides) yield but still remain intact. Zone III is the brittle-ductile transition zone. The morphology [Fig. 6(a)] shows severe cracks with many voids in zone III. This result indicates that the biaxial tensile stress (y - and z -axials) from the

triaxial state pulls away the material into x and y directions of this region to release the triaxial stress.

This type of fracture has not been reported previously on polycarbonate and why it occurs at this particular region is not completely clear now. Zones IV and V are the typical ductile tearing zones where the color of zone IV is relatively lighter, indicating more microshear yielding on the surface. After completion of this brittle-ductile transition zone, ductile tearing starts. The separation of zones IV and V

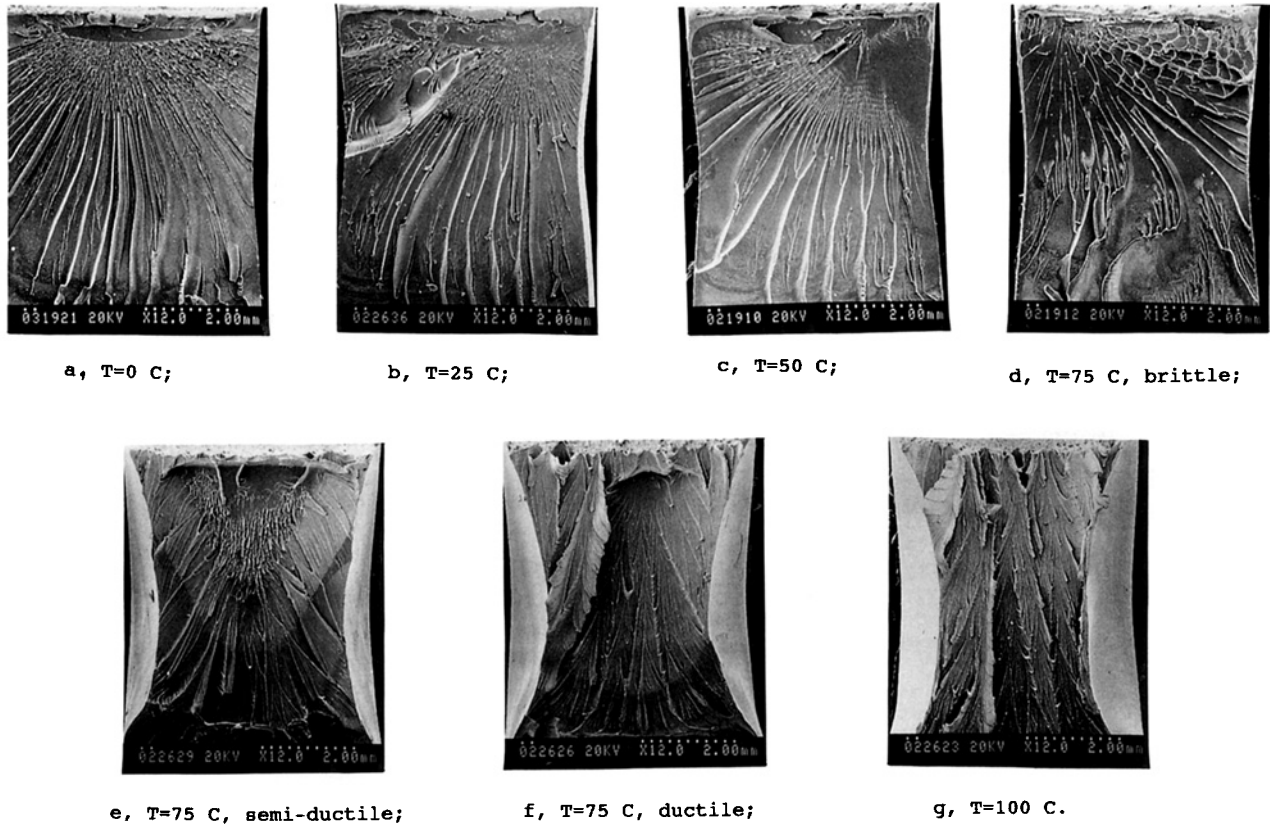


Figure 4 SEM photographs of polycarbonate fracture surfaces from specimens shown in Figure 2: (a) $T = 0^\circ\text{C}$; (b) $T = 25^\circ\text{C}$; (c) $T = 50^\circ\text{C}$; (d) $T = 75^\circ\text{C}$, brittle; (e) $T = 75^\circ\text{C}$, semiductile; (f) $T = 75^\circ\text{C}$, ductile; (g) $T = 100^\circ\text{C}$.

with a V-shaped curve [Fig. 6(b)] is not clear. We assume that this lighter zone is the slow grown plastic zone under relatively lower applied stress established during the time of the growing of zone III. At the beginning growing of zone IV, the stress of the plastic zone gets temporarily relief due to the strain energy release at the beginning of ductile tearing and the growth of the plastic zone front hesitates momentarily, then restarts. Zone VI is the unbroken zone and zone VII is the lateral constriction.

Precrack Hysteresis

Table II summarizes the results of the hysteresis studies by using four different load levels. Figure 7 shows the typical example of the load-displacement plots from four different loads prior to crack initiation (see curve F, Fig. 2). Both hysteresis energy (energy of the loop) and permanent displacement are increased with the increase of the applied load, as would be expected. Figure 8 illustrates the load-

displacement curves at constant load (30 kN) by varying testing temperatures. Both hysteresis energy and permanent displacement are increased with increase of temperature.

Figure 9 is another way of plotting to illustrate the effect of temperature on the resultant hysteresis energy. When the hysteresis energy is plotted against deformation displacement from four temperatures, a master curve can be obtained, as shown in Figure 10. Similar master curves using different molecular weights of polycarbonate and different amounts rubber in polycarbonate were also obtained.^{6,7} Figure 11 demonstrates the relationship between the precrack hysteresis energy and the resultant permanent displacement; the greater hysteresis energy results in higher permanent displacement. If the hysteresis precrack energy comes strictly from the viscoelasticity, the corresponding permanent displacement should be zero. Greater precrack hysteresis energy is indicative of greater precrack plasticity and thus a greater precrack plastic zone (contribution from crazes or microvoids in

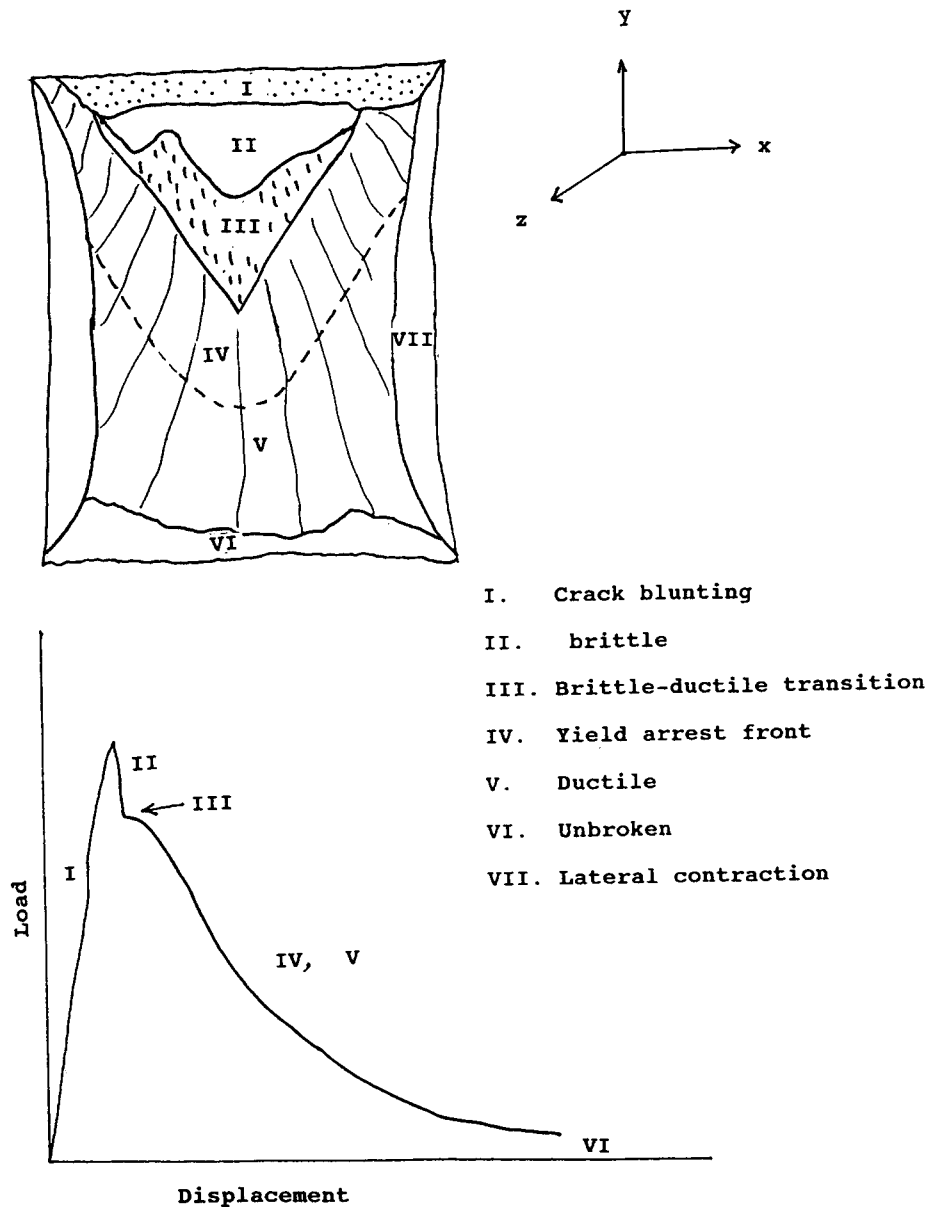


Figure 5 Replots of Figure 4(e) and the corresponding load-displacement curve.

this ductile material before crack initiation can be neglected). Therefore, a close relation exists between the precrack hysteresis energy and the size of the precrack plastic zone.

Comparative Hysteresis Energy vs. Displacement Curves

If we extrapolate this master curve shown in Figure 10 to intercept the y-axis at 2.5 mm deformation displacement, a hysteresis energy of about 0.17 J is obtained (Fig. 12). As mentioned earlier, this 2.5

mm is the critical brittle-ductile transition deformation displacement (L_c) for this system (Fig. 3). Figure 12 shows the replots of hysteresis energy vs. displacement curves from Figure 10 and from our previous articles based on varying molecular weight of polycarbonate⁶ and rubber content.⁷ The critical hysteresis energy from Figure 10 is actually identical to that determined from varying the polycarbonate molecular weight even though the L_c is higher at 3.1 mm.⁶ That means that the critical hysteresis energy for the brittle-ductile transition may be identical (or very close) for any polycarbonate system in spite

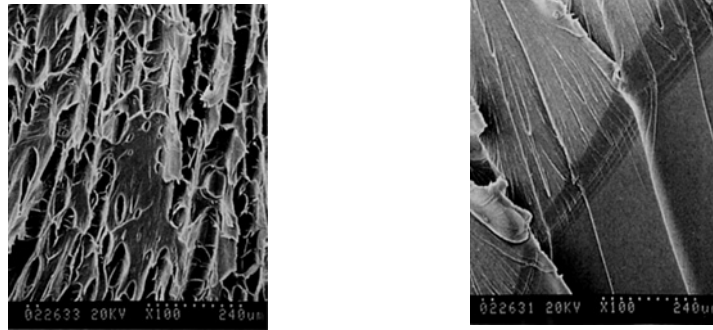


Figure 6 Detailed SEM photographs of Figure 4(e) and Figure 5: (a) zone III, brittle-ductile transition zone; (b) boundary line between zones IV and V of Figure 5.

of variation on the critical deformation displacement. If the above assumption is true or nearly true, the critical deformation displacement of the rubber-toughened polycarbonate system can be estimated at 2.73 mm (unobtainable experimentally, Ref. 7) (Fig. 12). That means that the same critical precrack plastic zone volume can be more effectively achieved at a lower deformation displacement by varying temperature, followed by varying rubber content, then by varying molecular weight. Un-

doubtedly, the change of yield stress plays a decisive role in dictating the resultant critical deformation displacement.

Effect of Precrack Elastic Storage Energy

This concept of critical precrack hysteresis energy (in terms of the corresponding critical precrack plastic zone volume) has been demonstrated as a viable approach to interpret the mechanism of the

Table II Summarized Hysteresis Data of Polycarbonate at Various Temperatures

Temp (°C)	Load (kN)	Displacement (mm × 10)	Permanent Displacement (mm × 10)	Total Energy (J × 10)	Hysteresis (%)	Hysteresis Energy (J × 10)
0	0.15	6.9	0.11	0.53	3.4	0.02
0	0.20	9.2	0.22	0.93	6.5	0.06
0	0.25	12.4	0.83	1.63	11.3	0.19
0	0.30	16.0	1.18	2.58	14.0	0.36
25	0.15	7.3	0.16	0.53	3.6	0.02
25	0.20	9.4	0.32	0.97	6.9	0.07
25	0.25	12.7	0.98	1.70	15.1	0.26
25	0.30	16.5	1.97	2.79	16.6	0.46
50	0.15	7.9	0.47	0.58	8.0	0.04
50	0.20	10.3	1.08	1.05	12.9	0.13
50	0.25	13.2	1.65	1.72	16.8	0.29
50	0.30	17.1	2.13	2.76	23.1	0.64
75	0.15	8.4	0.62	0.64	11.1	0.07
75	0.20	12.4	1.58	1.35	18.8	0.25
75	0.25	16.5	2.26	2.20	22.6	0.50
75	0.30	17.6	2.95	2.91	28.2	0.82
100	0.15	9.7	1.10	0.73	12.0	0.09
100	0.20	13.0	2.23	1.33	21.2	0.28
100	0.25	18.6	3.13	2.55	26.3	0.67
100	0.30	20.6	3.67	3.40	31.0	1.05

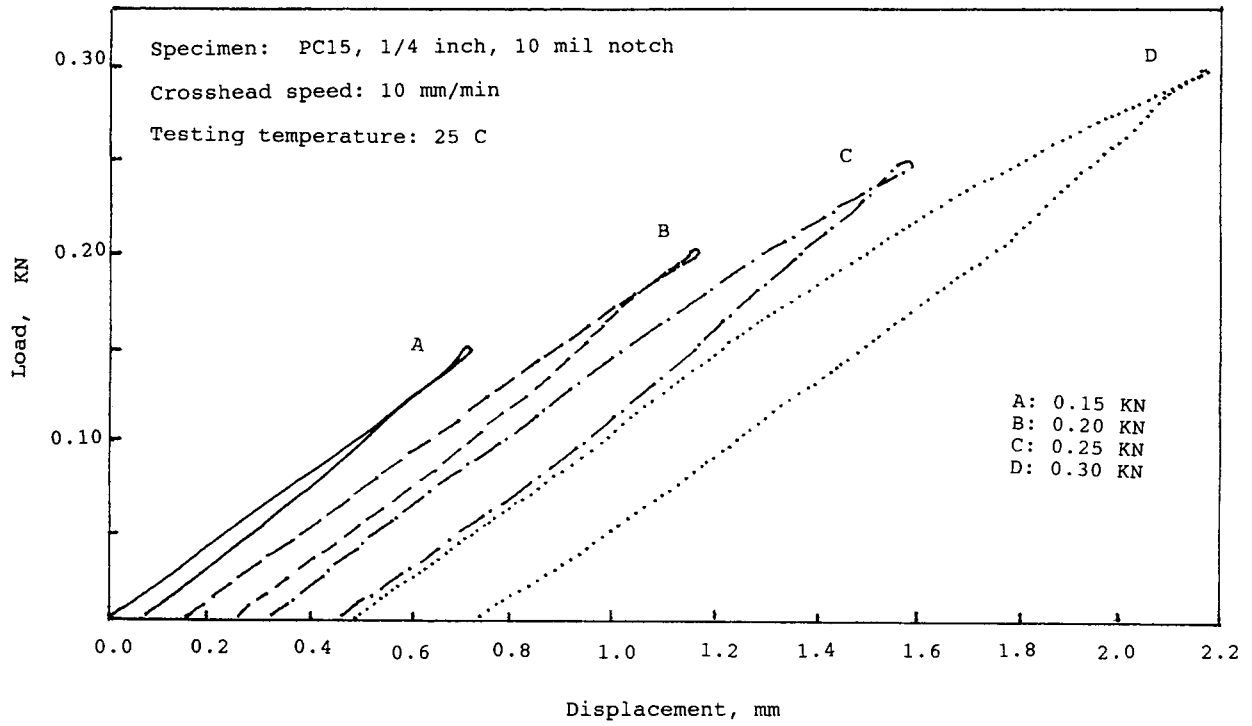


Figure 7 Load-displacement curves from the hysteresis cycles at four different load levels at 25°C.

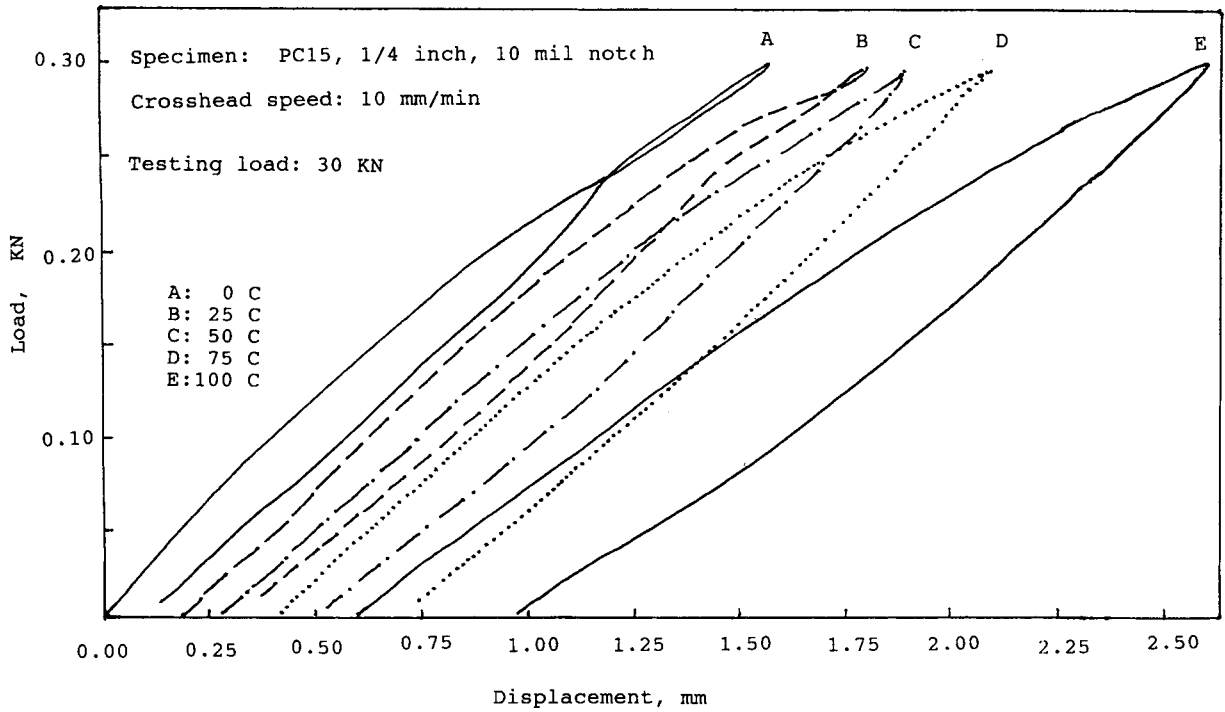


Figure 8 Load-displacement curves from the hysteresis cycles at different temperatures at a constant maximum load of 30 kN.

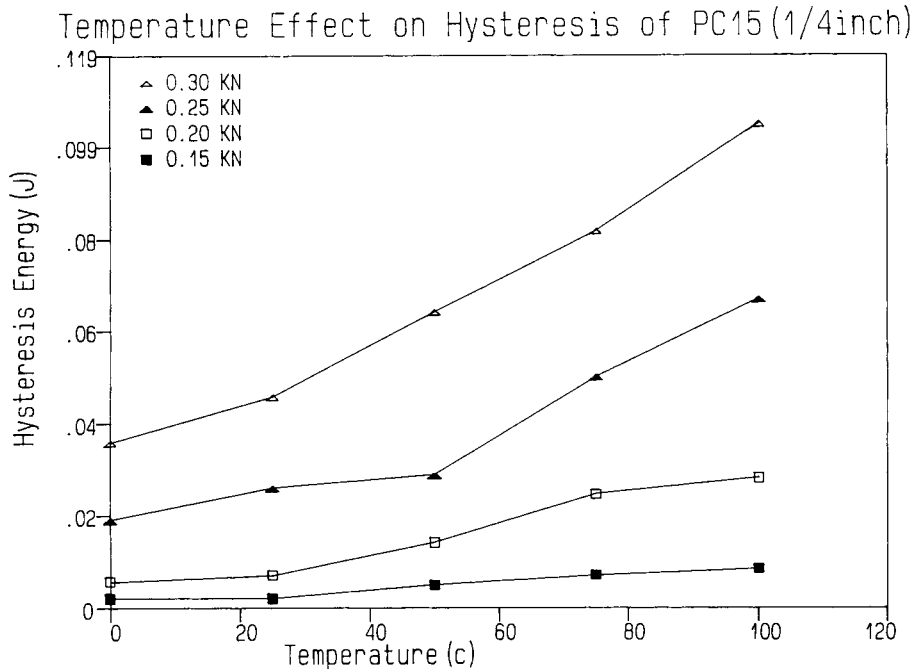


Figure 9 Relation of hysteresis vs. temperature under four different load levels.

observed brittle-ductile transition phenomenon. This proposed mechanism is based on the phenomenological observation but it is unable to give a clear reason why the changing of testing variable (or

varying material intrinsic properties) can affect the critical deformation displacement and results in either or ductile failure. As defined in the Theoretical Background section, the elastic storage energy is the

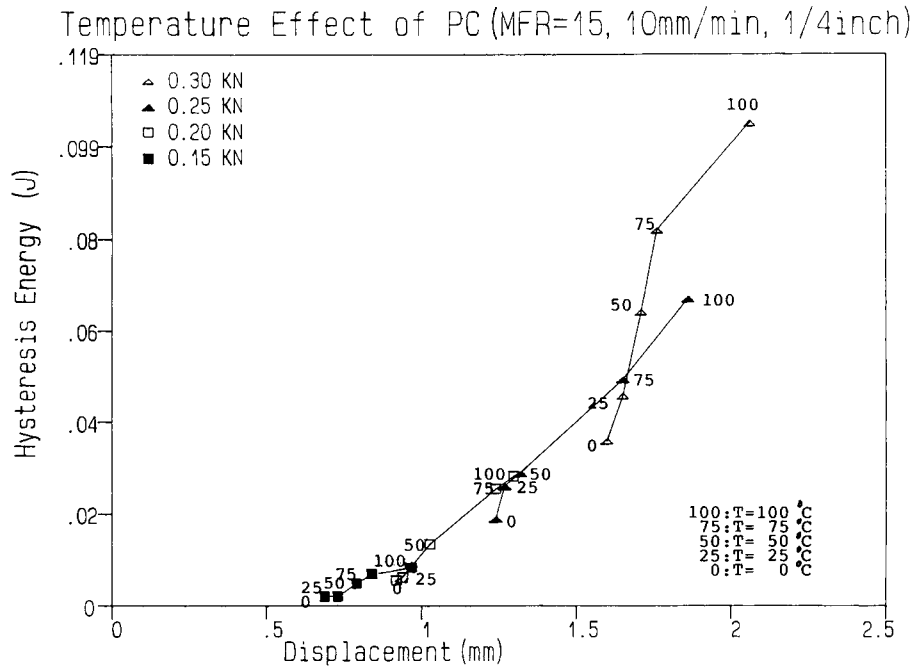


Figure 10 Relation of deformation displacement vs. precrack hysteresis energy from various load levels.

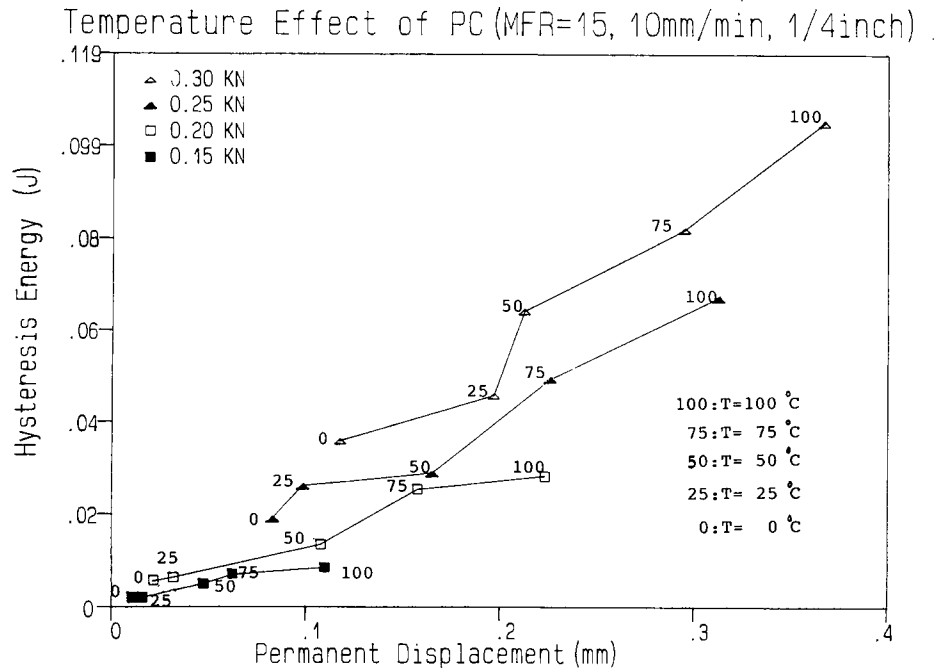


Figure 11 Relation of permanent displacement vs. precrack hysteresis energy from various load levels.

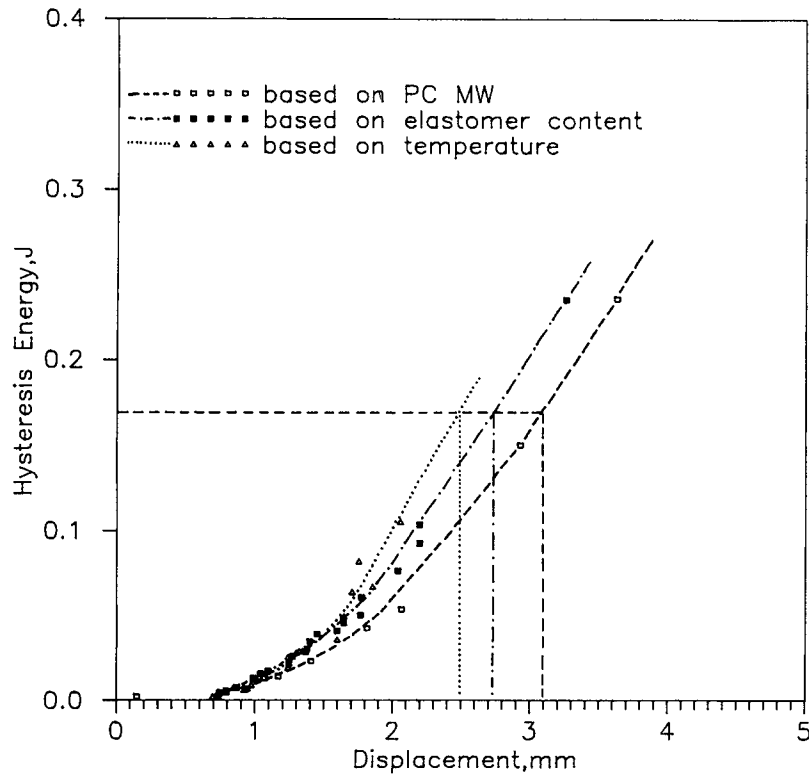


Figure 12 Master curves by plotting precrack hysteresis energy vs. deformation displacement: (A) ($\cdots\cdots\Delta\cdots\cdots$) varying testing temperatures (data from Fig. 10); (B) ($\cdots\cdots\blacksquare\cdots\cdots$) varying rubber contents in polycarbonate (data from Ref. 7); (C) ($\cdots\cdots\square\cdots\cdots$) varying polycarbonate molecular weights (data from Ref. 6).

total input energy minus the hysteresis energy. In the conventional plane-strain fracture mechanics, the precrack plasticity is virtually neglected and it is assumed that the input energy is the energy exclusively for crack initiation. In reality, especially for the toughened polymers, the precrack hysteresis energy (or inelastic energy) makes up a significant part of the input energy and certainly can no longer be neglected. The elastic storage energy is undoubtedly considered as the major driving force responsible for crack initiation. We did mention in our previous article⁷ that the presence of rubber in the rubber-toughened polycarbonates is able to reduce the input energy by converting portion of it into inelastic hysteresis and the elastic storage energy available for crack initiation is therefore reduced.

Figure 13 shows the extended plots of the storage energy vs. the deformation displacement under different temperatures where the temperature has a similar effect to that of the rubber presence to reduce the storage energy at any constant displacement. Figure 13 clearly demonstrates that the precrack storage energy increases with the decrease of testing temperature at a constant displacement. If we use the critical displacement for the brittle-ductile

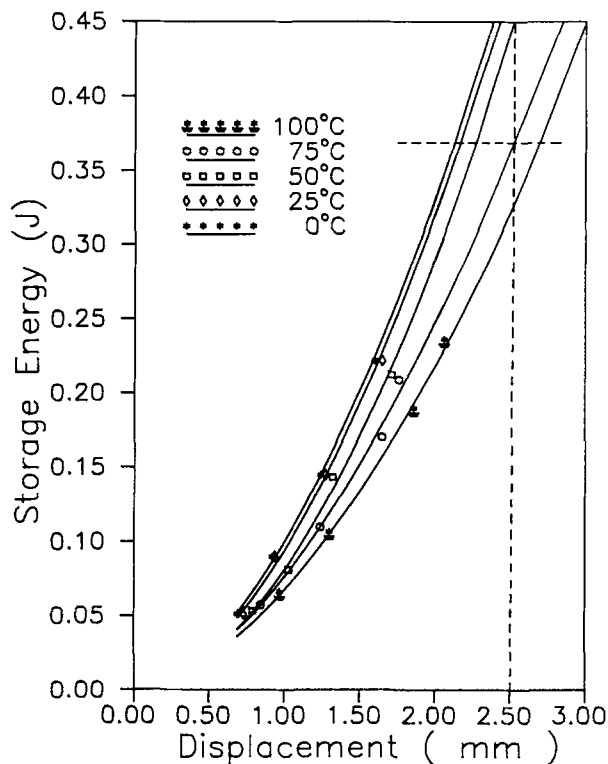


Figure 13 Plots of deformation displacement vs. precrack storage energy at various temperatures.

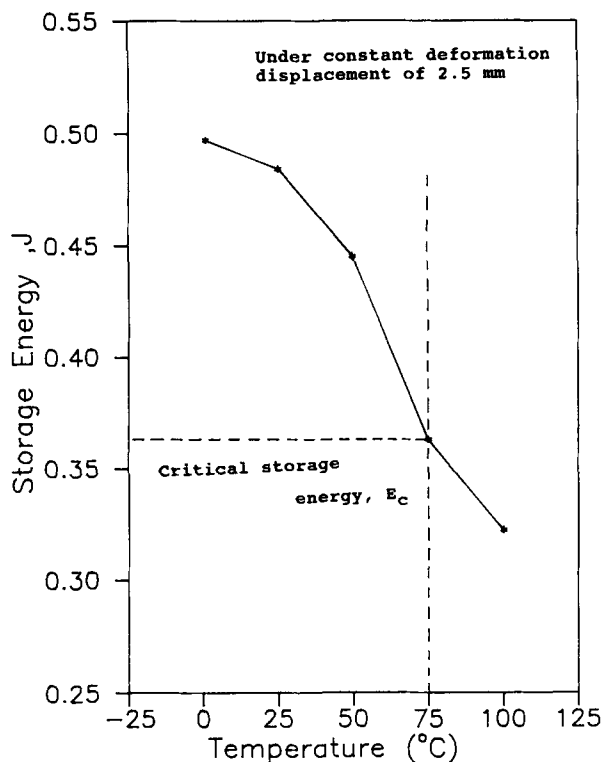


Figure 14 Temperature-dependent storage energy at critical deformation displacement, 2.5 mm.

transition determined from Figure 3 to intercept the curve in Figure 13, a relation of storage energy vs. temperature at the critical displacement can be obtained, as shown in Figure 14. Figure 14 clearly shows the importance of temperature in dictating the resultant storage energy and, therefore, the brittle-ductile transition, because the 0.36 J is the maximum allowable storage energy to resist crack initiation. If we take this 0.36 J storage energy line to intercept those curves in Figure 13, a relation of deformation displacement vs. temperature at this critical storage energy can be obtained, as shown in Figure 15. The deformation displacements between 2.1 and 2.3 mm are predicted for brittle crack initiations for temperatures from 0 to 50°C. This range of displacement is very close to the experimentally obtained brittle crack initiation displacements from Figure 3 and Table I.

The above data strongly emphasize that the elastic storage energy is the main driving force to induce crack initiation. More precrack plasticity at higher temperature diverts a greater fraction of the input energy into inelasticity and, therefore, reduces the elastic storage energy available for crack initiation. To reach the necessary storage energy for crack initiation, more input energy by further deforming the

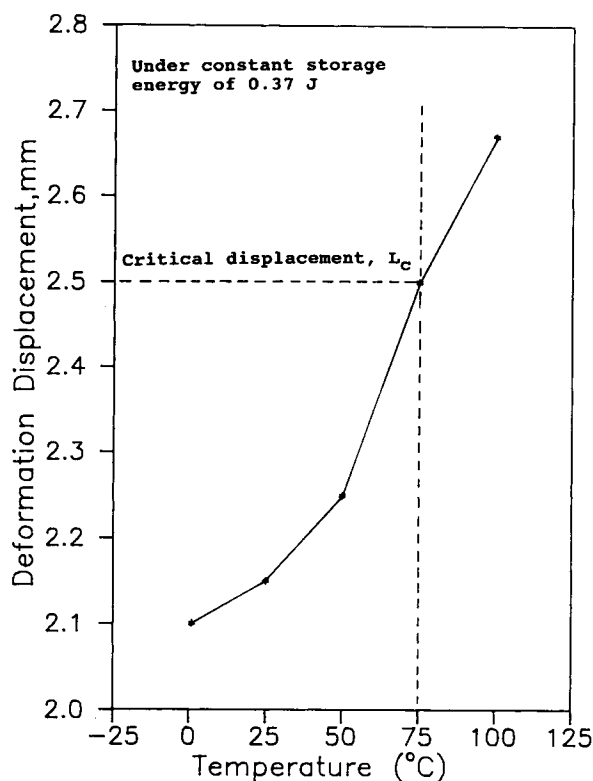


Figure 15 Temperature-dependent deformation displacement at critical storage energy, 0.37 J.

specimen is required. When the deformation displacement increases to its critical value, ductile fracture results.

CONCLUSIONS

This article continues our studies on the relationship between precrack hysteresis and its ductility in terms of the ductile–brittle transition behavior for polycarbonates. Results from this study based on a temperature variable provides further support to the previously proposed critical precrack plastic zone mechanism in determining the ductile–brittle transition behavior. Data also indicate that the precrack elastic storage energy is the major driving force in dictating the crack initiation. A minimum precrack storage energy (defined as input energy minus hysteresis energy) is required to strain the crack tip up to its endurance limit for the crack initiation. Higher temperature and the resulted lower yield stress can divert more fraction of the input energy into precrack plasticity and leaves relatively less elastic storage available to strain the crack tip for crack initiation. That means that additional input energy

and therefore longer deformation displacement is necessary to build up the precrack elastic storage up to its critical level for the crack initiation. Other variables, such as deformation rate, notch radius, annealing, molecular weight distribution, directionality, and cooling rate, used to correlate the precrack hysteresis and their corresponding ductility in terms of ductile–brittle transition behavior, will be reported later.

The authors are grateful to the National Science Council of the Republic of China for financial support.

REFERENCES

1. E. H. Andrews, *Fracture in Polymers*, American Elsevier, New York, 1968.
2. S. Wu, *Polym. Eng. Sci.*, **30**, 72 (1990).
3. R. P. Kambour, *Polym. Commun.*, **24**, 292 (1983).
4. I. M. Ward, *Mechanical Properties of Solid Polymers*, 2nd ed., Wiley, Chichester, UK, 1983, pp. 432–436.
5. F. C. Chang, J. S. Wu, and L. H. Chu, *J. Appl. Polym. Sci.*, **44**, 491 (1992).
6. F. C. Chang and H. C. Hsu, *J. Appl. Polym. Sci.*, **43**, 1025 (1991).
7. F. C. Chang and H. C. Hsu, *J. Appl. Polym. Sci.*, **47**, 2195 (1993).
8. F. C. Chang, *Handbook of Advanced Materials Testing*, Marcel Dekker, Matawan, NJ, to appear.
9. C. B. Lee and F. C. Chang, *Polym. Eng. Sci.*, **32**, 192 (1992).
10. C. B. Lee, M. L. Lu, and F. C. Chang, *J. Appl. Polym. Sci.*, **47**, 1867 (1993).
11. C. B. Lee, M. L. Lu, and F. C. Chang, *J. Chin. Inst. Chem. Eng.*, **23**, 305 (1992).
12. F. C. Chang and M. Y. Yang, *Polym. Eng. Sci.*, **30**, 543 (1990).
13. F. C. Chang, J. S. Wu, and M. Y. Yang, *Polymer*, **32**, 1394 (1991).
14. F. C. Chang and Y. C. Hwu, *Polym. Eng. Sci.*, **31**, 1509 (1991).
15. R. A. W. Fraser and I. M. Ward, *J. Mater. Sci.*, **12**, 459 (1977).
16. A. F. Yee, *J. Mater. Sci.*, **12**, 757 (1977).
17. M. E. J. Dekkers and S. Y. Hobbs, *Polym. Eng. Sci.*, **27**, 1164 (1987).
18. F. C. Chang and L. H. Chu, *J. Appl. Polym. Sci.*, **44**, 1615 (1992).
19. W. B. Liu and F. C. Chang, in *Proceedings of the 15th ROC Polymer Symposium*, Taiwan, 1992, p. 215.
20. R. C. Chen and F. C. Chang, *Polym. Networks Blends*, **3**, 107 (1993).
21. I. Narisawa and M. T. Takemori, *Polym. Eng. Sci.*, **28**, 1462 (1988).

Received October 20, 1993

Accepted December 30, 1993